European Journal of Research Development and Sustainability (EJRDS)
Available Online at: https://www.scholarzest.com
Vol. 3 No. 9, September 2022
ISSN: 2660-5570

MODELING OF CODE TRANSMISSION PROCESS OF MICROELECTRONIC TRANSMITTER RELAYS

Aripov N.M.
Doctor of Technical Sciences,
Mirzarakhmedov Z.F
Tashkent State Transport University, 1 Temiryulchilar Str., Tashkent 100069, Uzbekistan

Article history:

Received: 17th July 2022
Accepted: 17th July 2022
Published: 30th September 2022

Abstract:

At present, microprocessor and microelectronic systems and devices are widely used in railway automation and remote control systems. The use of systems and devices for railway automation and remote control, developed on the basis of microelectronics and microprocessor elements, ensures reliable operation in comparison with systems based on electromagnetic relays. The process of using and maintaining microelectronic and microprocessor systems is simplified.

Currently , the joint-stock company «Uzbekistan Temir Yollari» is using a new type of microprocessor auto-locking systems and semi-auto-locking systems. However, most of the railway sections of the joint-stock company «Uzbekistan Temir Yollari» are composed of relay automatic blocking and semi-automatic blocking systems. In this article, the process of modeling the principles of operation of the transmitter relays designed to transmit the codes formed by the KPTSH transmitter to road traffic lights and locomotive traffic lights in rail chains equipped with AB systems and automatic locomotive signaling systems is considered based on Petri nets. The newly developed integrated microprocessor code transmitter for the transmission of codes formed in railway automation and telemechanics systems has been studied the process of transmission of «G» codes (for green colour codes) . Time descriptions of pulses of TSH-65 and TSH-2000 transmitter relays, as well as diagrams of time descriptions of pulses and intervals in «G" code for transmitter relays.

Keywords: Autoblocking, locomotive automatic signaling, electrical centralization systems, rail chains, code, processes, anchor, relay, Petri nets, graphs.

INTRODUCTION

TSH-65 and TSH-2000 relays undertake the function of code transmission in railway automation and telemechanics (RAT). As a result of the evolution of time and increasing requirements for road safety, these devices also need to be updated.[1-14].

The theory of Petri nets makes it possible to model RAT systems in the form of Petri nets in a mathematical hypothesis. The theory of Petri nets serves to model several parallel processes occurring simultaneously in systems.

RESEARCH FOR THE» G « CODE IN PETRI SCANS IN MODELING.

Time diagrams of TSH transmitter relays during code transmission, one pulse is one interval for «Red and Yellow – RY codes» , two pulses are two intervals for «Yellow» code, three pulses are three intervals for «G» code. The duration of pulses and intervals consists of special periods for codes. Below we will get acquainted with how the Petri graphs for the «G» code are expressed [15-20].

Processes (P), conditional transitions (T), input (I) and output (O) are the basis of Petri nets. Processes and conditional transitions are interconnected by the execution of tasks that enter or exit these processes and transitions. Graphs are used to simplify Petri nets in research. These graphs are represented as multigraphs in the Petri simulator.

Based on this, in Petri plots -processes of logical elements namely it's states, -and logical element means conditional jumps. To specify which process is active in Petri nets, it is used logical sign - is determined by placing a checker in the circle [15,16].

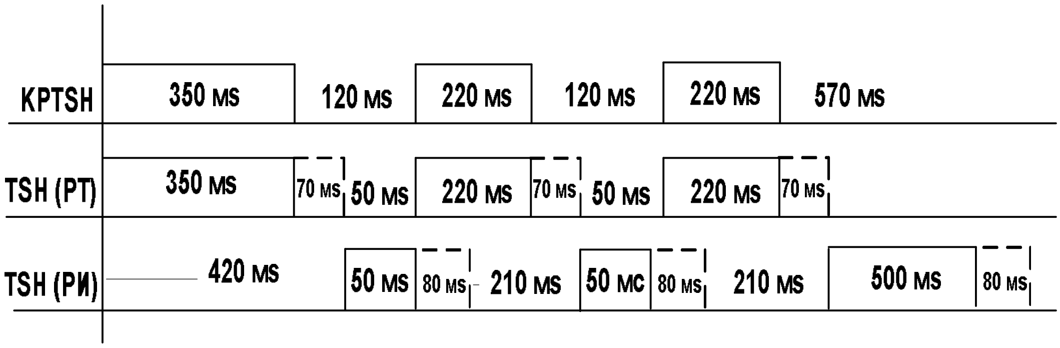

Figure 1. Diagram of the timing characteristics of pulse intervals in the code «G» for relay-transmitters TSH-65 and TSH-2000

Table 1 lists the processes and descriptions of processes in Petri nets for code «G»

Table 1

Order of proceedings	**Purpose of the procedure**
P1	The supply was given and the impulse started to come.
P2	Dropping of PT relay armature .
P3	The process of checking the arrival of a pulse for 350 MS (milliseconds).
P4 P11 P15	PT relay anchor drops during the interval after the pulse ends expiration of the delay time in 70 MS.
P5	During the pulse, the process of raising the armature of the PT relay.
P6 P12	Interval process for 50 MS.
P7	Dropping of PИ relay anchor.
P8 P13 P17	80MS delay time for pulse arrival and PИ relay armature drop out after interval timeout check process.
P9 P14	Pulse arrival and PИ relay armature delay of 80 MS and pulse arrival process of 220 MS.
P10	The rise of PИ relay armature.
P16	Interval arrival process for 500 MS
Order of conditions	**Assigning transition conditions**
t1	Start receiving pulse 0÷350MS
t2 t6 t10	Checking the transition condition to the interval after the end of the impulse.
t3 t7 t11	After the 70 MS delay, the armature of the PT relay switches from the energized state to the de-energized state.
t4 t8	Checking of the 50 MS interval continues after the 70 MS delay time.
t5 t9	Checking the start of the 80 MS delay after the 50 MS interval.
t12	Checking of the 500 MS interval comes after the 70 MS delay.
t13	Checking of 80MS delay timeout and RI relay switching to no current state.

The graph consists of transitions t1, t2, …….. and t22 and processes P1, P2 …….. and P17.

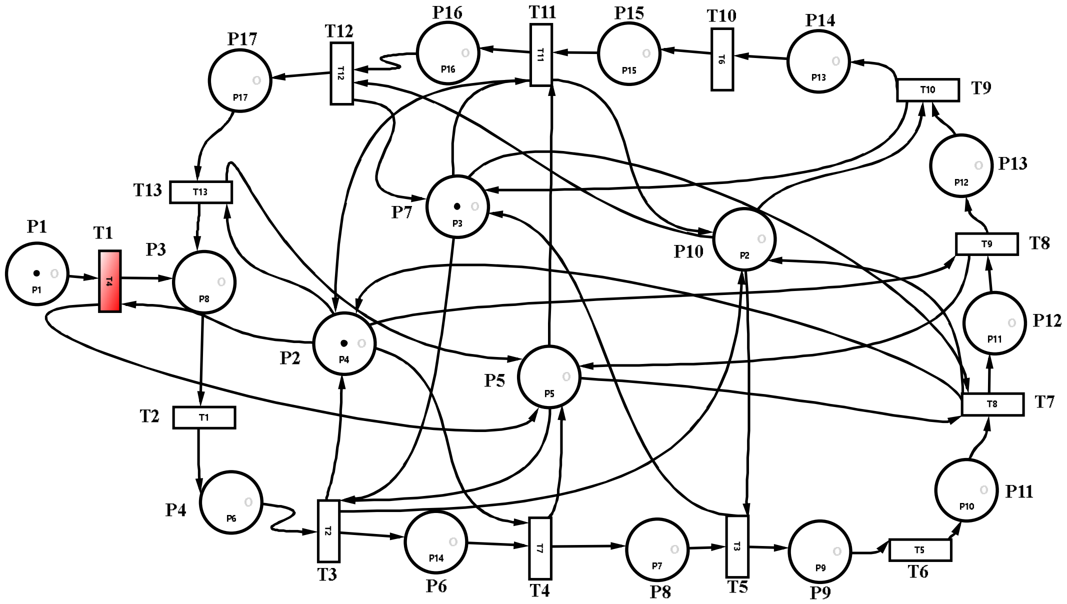

Figure 2. «G» code TSH transmitter relays start state when supply is connected

Graph representation of Petri net

A power-on pulse activates process P1. As a result of the fulfillment of the condition for the arrival of a pulse for a period t1 350 MS, we obtain outputs O(t1) = {P3, P5} (Fig. 2).

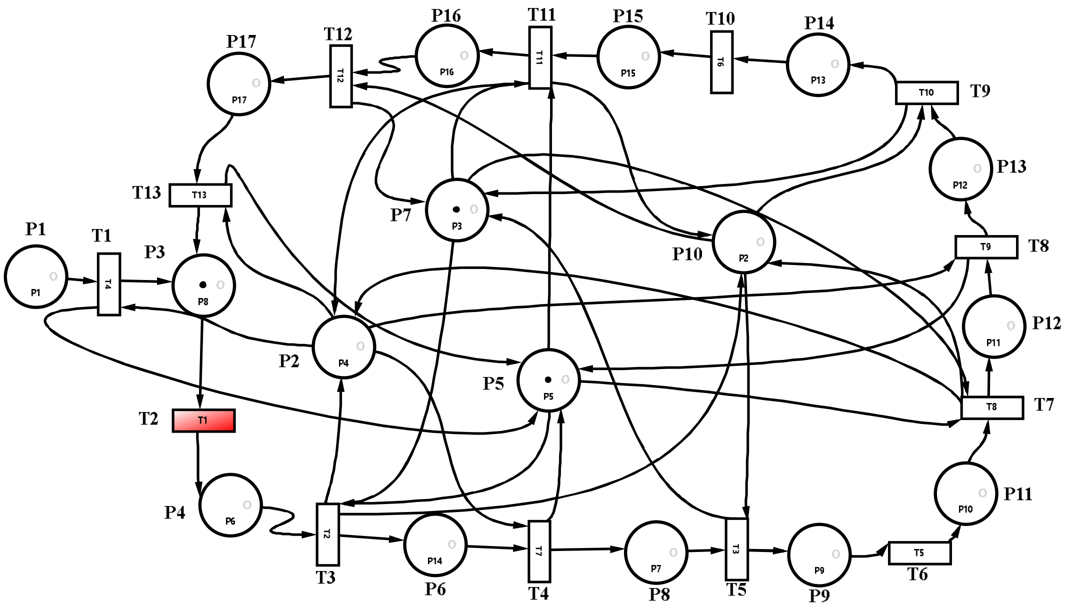

Figure 3. TSH transmitter relays for «G» code when the power supply is connected 0÷350 MS pulse receiving state representation of the Petri net graph.

Outputs O(t1) = {P3, P5} activate the processes shown in Figure 3. Process P3 is used to transfer the armature of the relay PT to the current state as a result of the condition t1. And the P5 process controls the process of the pulse input to the PT armature for 0÷350 MS. 350 MS after the input of the pulse on arrival, I(t2)={P4} checks the condition for the beginning of the interval after the end of the input pulse (Figure 3).

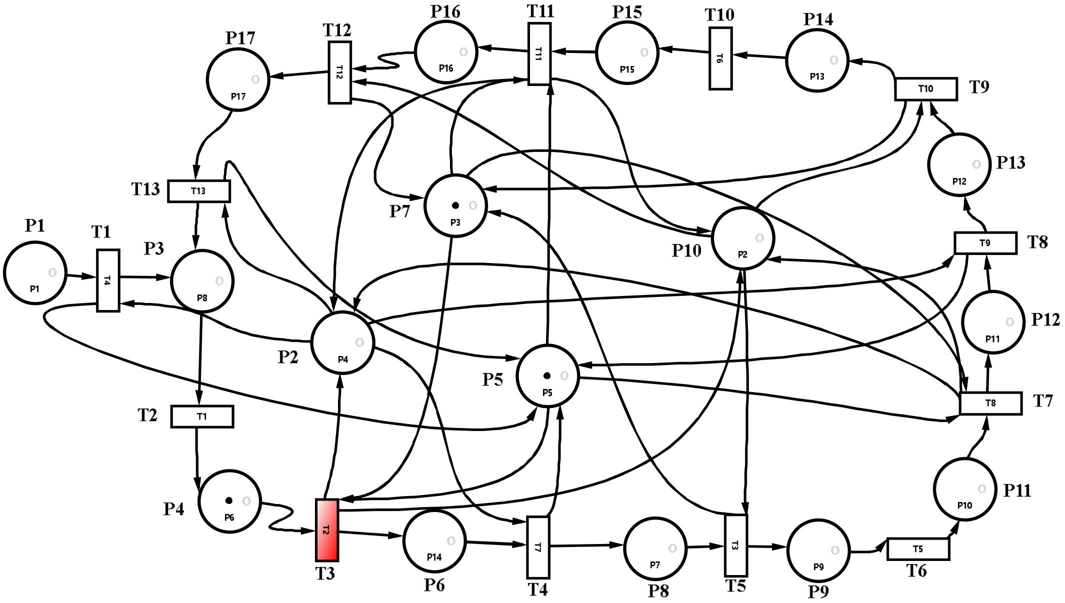

Figure 4. Petri net plot of 70MS delay process testing PT anchor drop for code «G».

Figure 4 shows that the delay time of 70 MS for the execution of the input data I(t3)={P6,P10} to release the PT armature due to the activation of the P4 process has ended.

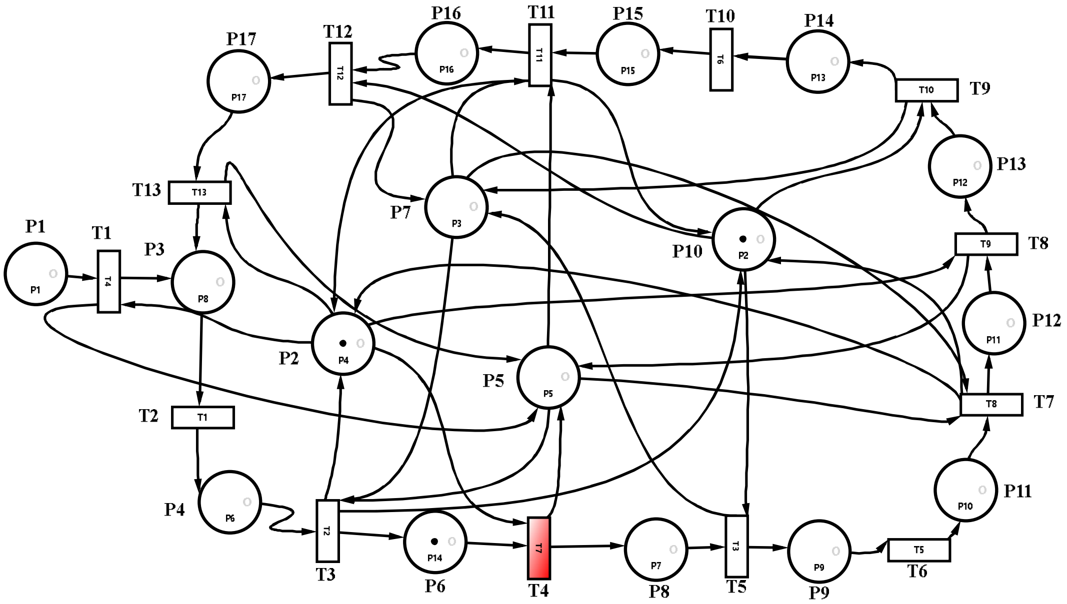

Figure 5. Petri net plot of PT anchor drop and 50 MS interval for code "G".

In Figure 5, generating output O(t3)={P2} results in a token in process P2, which represents the fall of the PT armature. O(t3)={P6} passes through the chip to process P6. And in this process there is a time interval of 50 ms.

A total of 120 ms of latency and interval time ensures that the interval is fully implemented. The end of the interval sets the stage for the start of the next impulse process via the output O(t4)={P5}(Fig. 6).

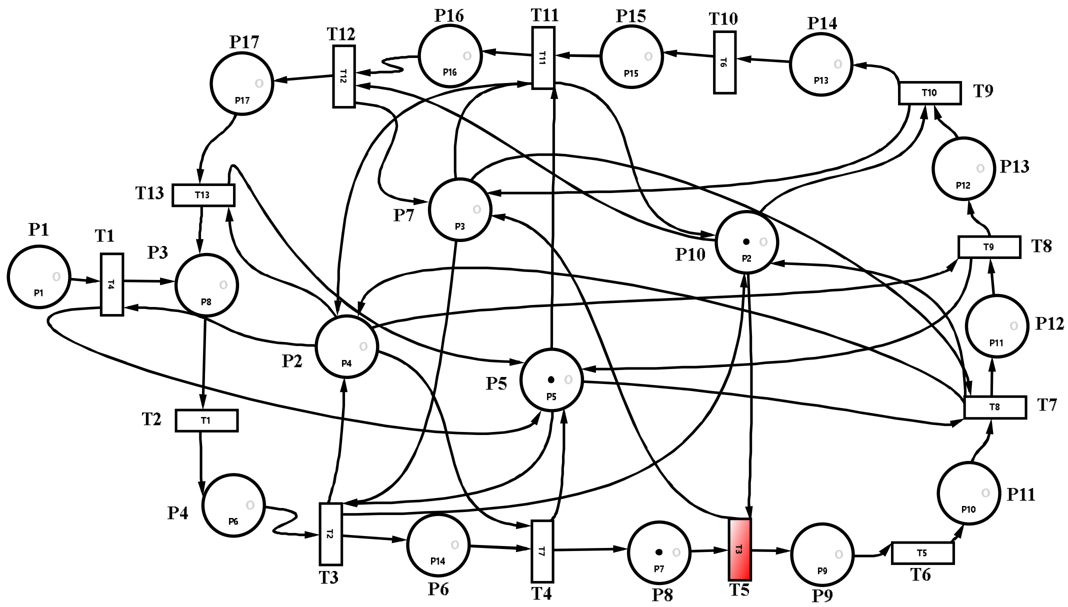

Figure 6. PИ anchor rise for «G» code Petri net graph

When O(t4)={P8} output occurs, the t5 condition controls the interval and the 80MS interval delay start condition. After that, process P7 and P9 is activated with output O(t5)={P7,P9}. The appearance of a microcircuit on P9 starts the process of entering a pulse for 220 MS (Fig. 7).

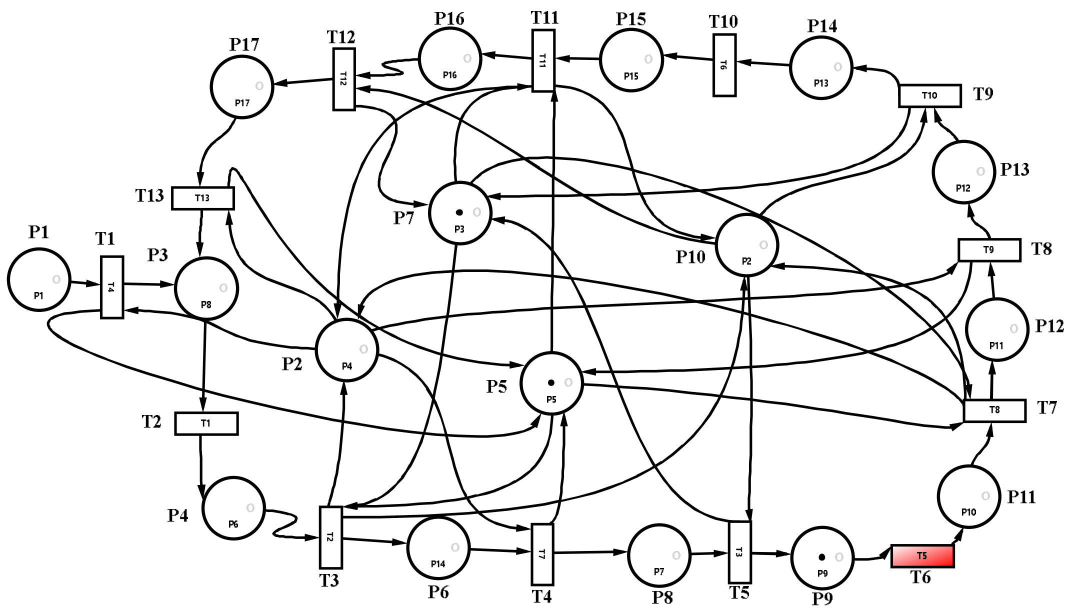

Figure 7. Delay time for PИ anchor drop for «G» code Petri net graph

Figure 7 shows the process of fulfilling the condition of the delay time for the PИ anchor to drop as a result of the activation of the process P7 through the input I(t6)={P9}.The presence of input data I(t5)={P8,P10} indicates that the delay of 80 MS has ended. The fulfillment of the condition t8 activates the process P9, the appearance of a flash in the process P9 is considered evidence that the armature PИ has passed from the on state to the de-energized state. Therefore, the first impulse and the interval come to an end. O(t4)={P8} indicates that the second pulse has started.

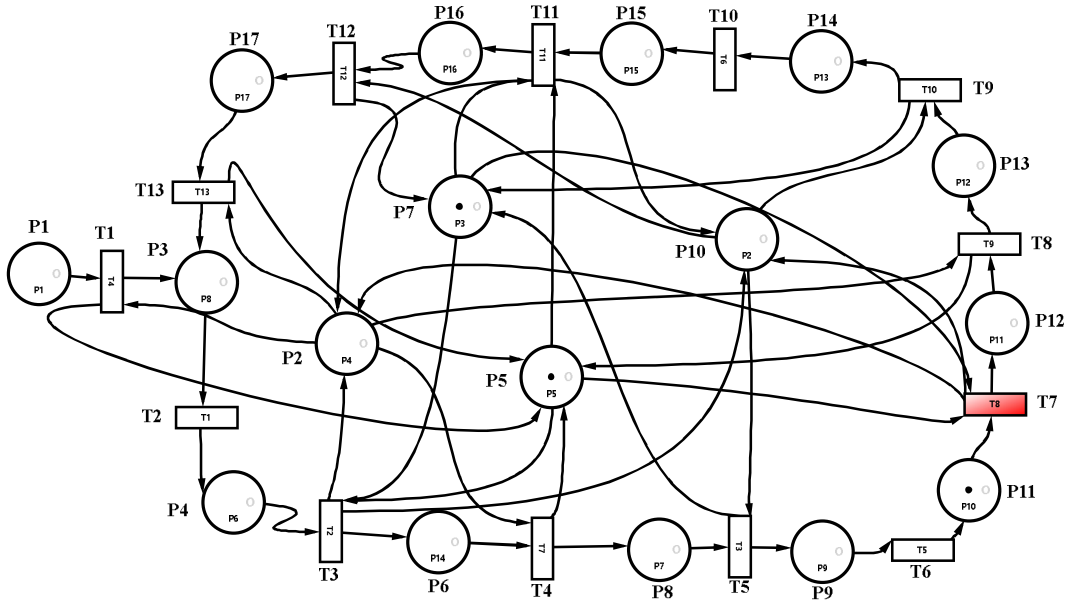

Figure 8. Graph of the Petri net showing the beginning of the 2nd cycle and the arrival of the pulse between 470 ÷ 690 MS for code «G»

The activation of process P11 indicates that the reception of pulses has begun. Activation of the P12 process serves to lift the PT anchor. The transition of the PT armature to the current state is a process of an incoming pulse with a duration of 220 MS (Fig. 8).

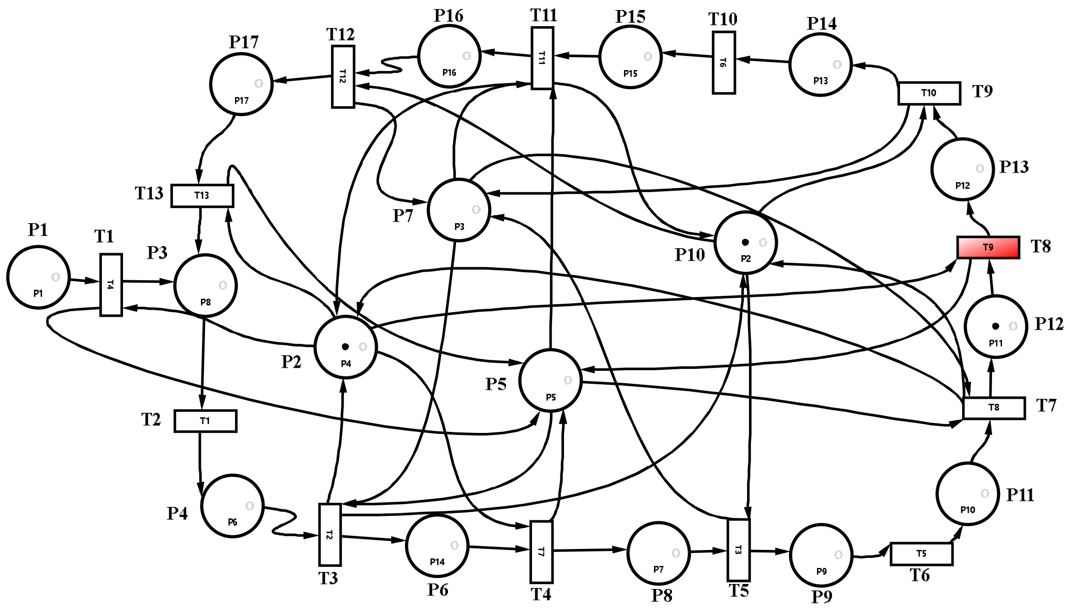

Figure 9. Plot of the Petri net of the transition of the PT armature from the energized state to the de-energized state for code «G».

In Figure 9, output O(t6)={P11} is generated and P11 is activated. As a result, the PT lowers the anchor. The transition of the PT from the on state to the de-energized state means the end of the pulse in the second cycle. Activating P12 causes the interval to last 50 ms and input I(t8)={P12}.

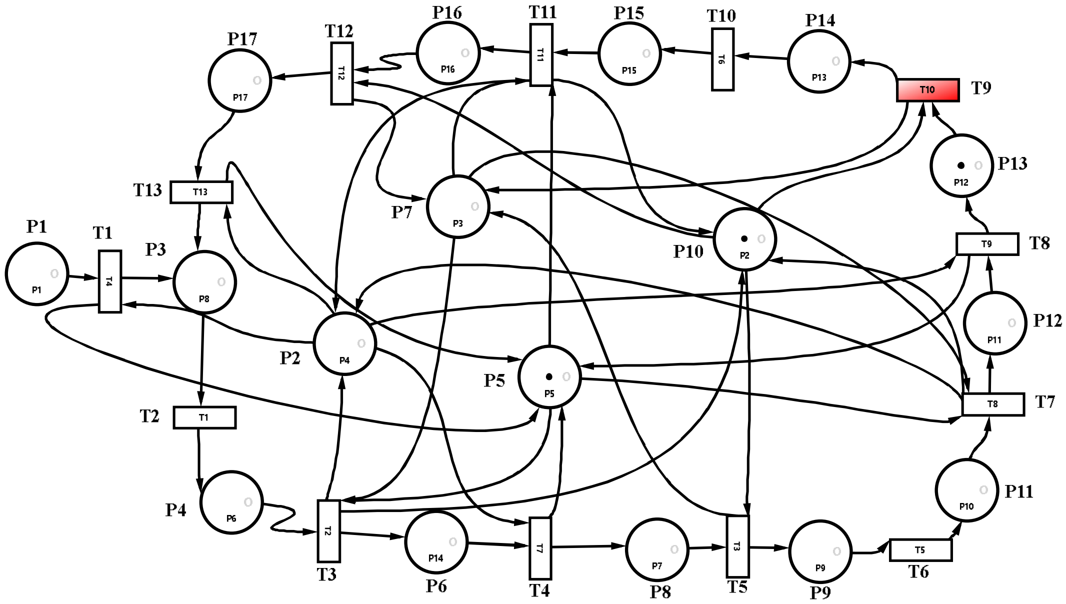

Figure 10. . Petri net plot of PИ anchor transition from dead to live for G code.

Generation of output data O(t7)={P10} serves to raise the PИ anchor. And the input I(t8)={P12} checks the interval condition for 50 MS(Figure 10).

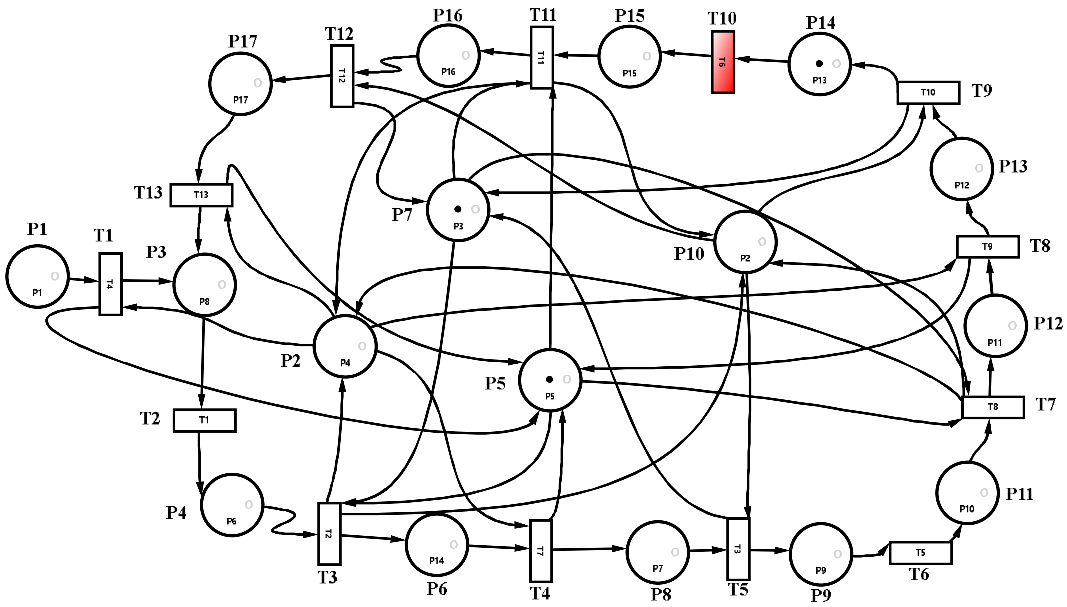

Figure 11. Petri net plot of the current to uncurrent PИ anchor transition for code «G».

Figure 11 illustrates the 80MS delay that goes into lowering the PИ anchor in process P16 via output O(t8)={P13}.The execution of this process generates the input I(t9)={P10,P13} and checks the conditions for the transition of the t9 PИ armature from the on state to the de-energized state. Therefore, after the interval and delay time has elapsed, process P7 is activated, and the switchgear armature goes into the open state. Therefore, the second impulse and the interval come to an end.

The appearance of the output O(t8)={P13} means that the process of the third impulse has begun. The chip appears in the process P14 through the output O(t9)={P14}.

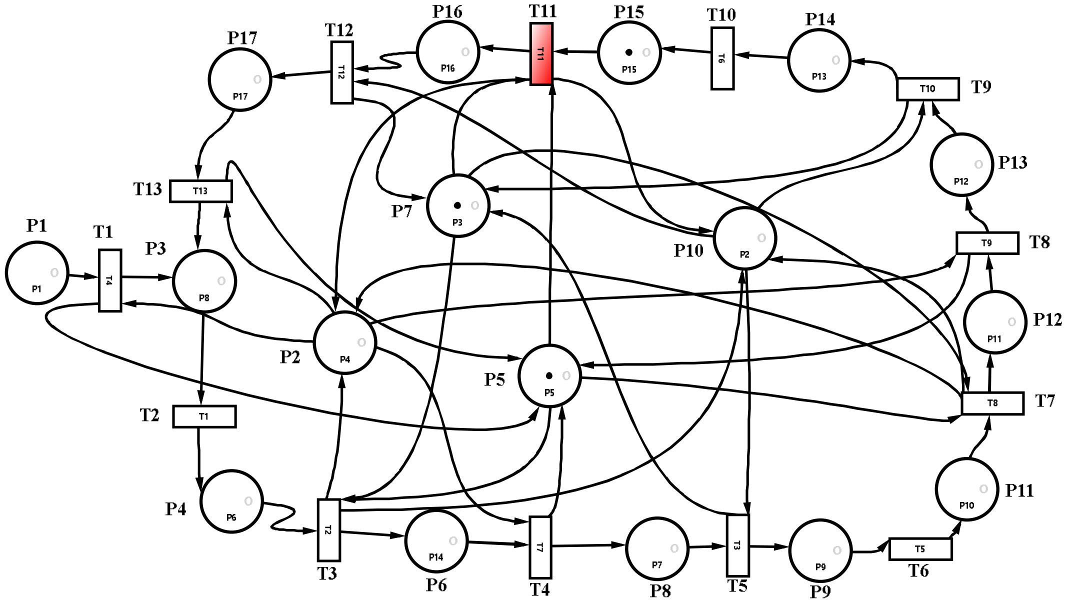

Figure 12. Petri net graph of pulse arrival for 810÷1030 MS for «G» code.

O(t9)= {P14} in process P14 via output 810÷1030 MS interval indicates that the pulse is present. (t10)={P15} outputs a 70ms delay to drop the RT anchor in process P15. (Fig. 12).

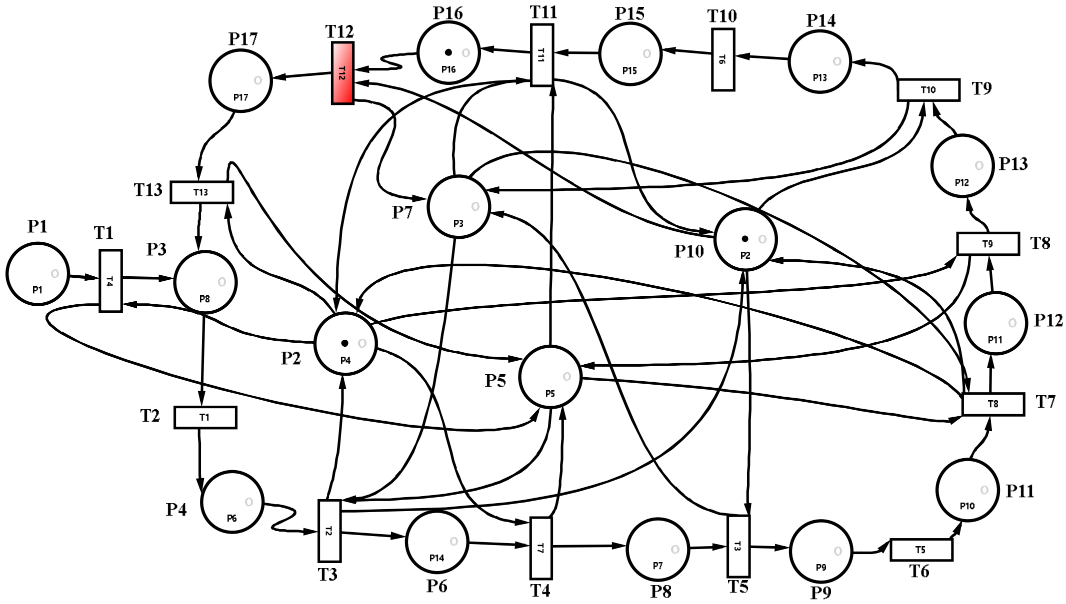

Figure 13. Plot of the Petri net of the transition of the PT anchor from on to off for the code «G»

After checking that the impulse came completely through the conditional t11, we get the input I(t11)={P5,P15}. This, in turn, activates process P2 to switch the armature PT from the on state to the de-energized state. Through the output O(t11)={P16} in the process P16, the interval of 500 MS begins (fig. 13).

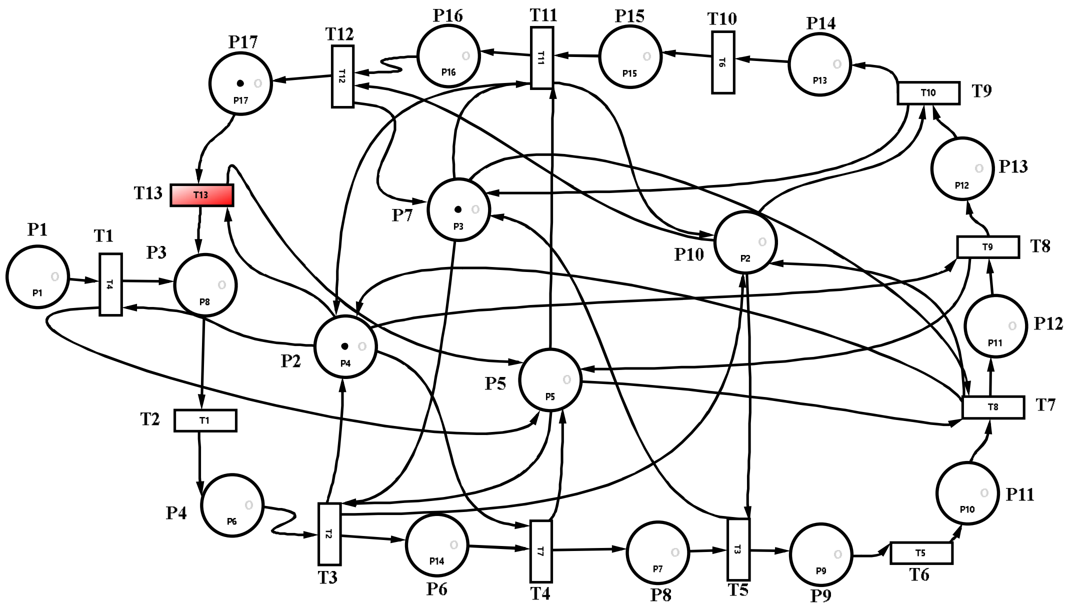

Figure 14. Graph of the Petri net of the transition of the РИ armature from a de-energized state to on for the code «G»

Figure 14 shows the transition to the current state due to the rise of the armature РИ in the process of P10 through the output O(t11)={P10}.As a result of exit O(t11)={P16} process P16 is activated represented by interval 1100÷1600 MS.

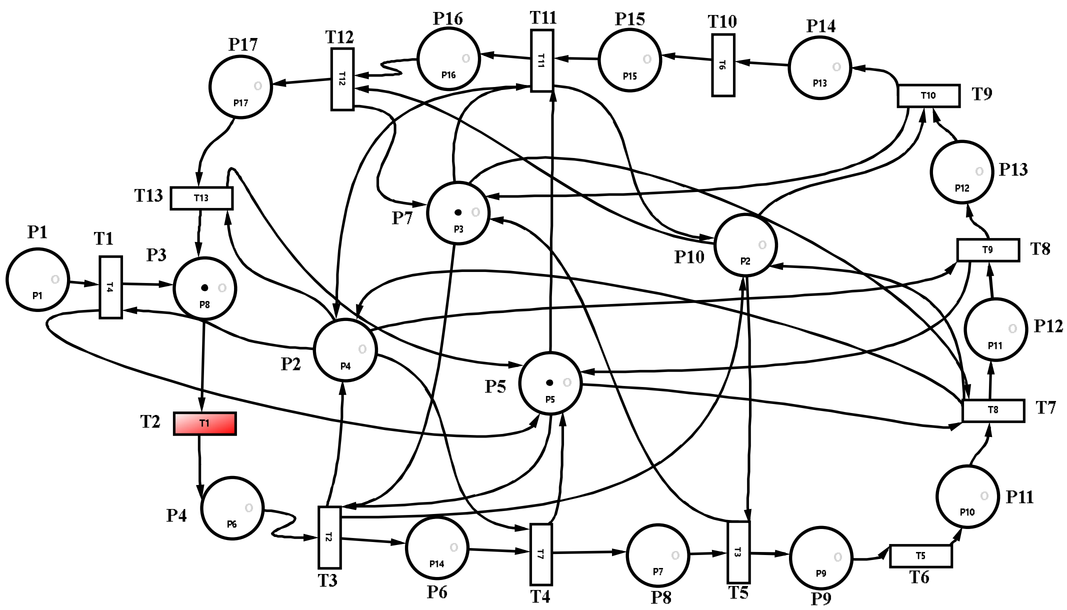

Figure 15. Plot of the Petri net after three impulses and three intervals for the code «G».

The appearance of the inputs I(t13)={P17,P10} activates the check of the end of the interval and return to the initial state. O(t13)={P3} activates process P3 via exit. Which, in turn, is equal to 0÷350. When organizing the arrival of through the impulses and intervals for the code «G» mean that the sequence of arrivals starts again from the beginning of Fig. 15 .

The fulfillment of the condition t12 leads to the output O(t22)={P7} in addition to the output O(t12)={P17}. As a result, the P17 process is activated, and after the delay time of 80 MS for the fall of the РИ armature, the РИ armature is de-energized, thereby completing the third interval .

Extended input (I) and output (O) functions for the Petri graph in the code «G» of the TSH-65 relay are presented in Table 2.

Table 2

I(t1)={P1,P5}	*O(t1)={P3,P5}*
I(t2)={P3}	*O(t2)={P4}*
I(t3)={P4,P5,P7}	*O(t3)={P2,P6,P10}*
I(t4)={P2,P4}	*O(t4)={P5,P8}*
I(t5)={P8,P10}	*O(t5)={P7,P9}*
I(t6)={P9}	*O(t6)={P11}*
I(t7)={P5,P7,P11}	*O(t7)={P2,P10,P12}*

I(t8)={P2,P12}	*O(t8)={P5,P13}*
I(t9)={P10,P13}	*O(t9)={P7,P14}*
I(t10)={P14 }	*O(t10)={P15}*
I(t11)={ P5,P7,P15 }	*O(t11)={P2,P10,P16}*
I(t12)={P10,P16}	*O(t12)={P7,P17}*
I(t13)={P12,P17}	*O(t13)={P3,P5}*

Corresponding to the expression in Table 2, the expression forms a matrix of shapes 1 and 2.

$$i_{j\varepsilon} = \begin{cases} 1, agar \to p_\varepsilon \in P^I t_j \cup t_j \in T^0 p_\varepsilon, \\ 0, agar \to p_\varepsilon \notin P^I t_j \cap t_j \notin T^0 p_\varepsilon \end{cases}$$

$I = |t_{\tau\varepsilon}| =$

P1	P2	P3	P4	P5	P6	P7	P8	P9	P10	P11	P12	P13	P14	P15	P16	P17	
0	0	0	0	0	0	0	0	0	0	0	0	0	0	0	0	0	t1
0	0	0	0	0	0	0	0	0	0	0	0	0	0	0	0	0	t2
0	0	0	0	0	0	0	0	0	0	0	0	0	0	0	0	0	t3
0	0	0	0	0	0	0	0	0	0	0	0	0	0	0	0	0	t4
0	0	0	0	0	0	0	0	0	0	0	0	0	0	0	0	0	t5
0	0	0	0	0	0	0	0	0	0	0	0	0	0	0	0	0	t6
0	0	0	0	0	0	0	0	0	0	0	0	0	0	0	0	0	t7
0	0	0	0	0	0	0	0	0	0	0	0	0	0	0	0	0	t8
0	0	0	0	0	0	0	0	0	0	0	0	0	0	0	0	0	t9
0	0	0	0	0	0	0	0	0	0	0	0	0	0	0	0	0	t10
0	0	0	0	0	0	0	0	0	0	0	0	0	0	0	0	0	t11
0	0	0	0	0	0	0	0	0	0	0	0	0	0	0	0	0	t12
0	0	0	0	0	0	0	0	0	0	0	0	0	0	0	0	0	t13

Matrix 1

$O = |t_{\tau\varepsilon}| =$

P1	P2	P3	P4	P5	P6	P7	P8	P9	P10	P11	P12	P13	P14	P15	P16	P17	
0	0	0	0	0	0	0	0	0	0	0	0	0	0	0	0	0	t1
0	0	0	0	0	0	0	0	0	0	0	0	0	0	0	0	0	t2
0	0	0	0	0	0	0	0	0	0	0	0	0	0	0	0	0	t3
0	0	0	0	0	0	0	0	0	0	0	0	0	0	0	0	0	t4
0	0	0	0	0	0	0	0	0	0	0	0	0	0	0	0	0	t5
0	0	0	0	0	0	0	0	0	0	0	0	0	0	0	0	0	t6
0	0	0	0	0	0	0	0	0	0	0	0	0	0	0	0	0	t7
0	0	0	0	0	0	0	0	0	0	0	0	0	0	0	0	0	t8
0	0	0	0	0	0	0	0	0	0	0	0	0	0	0	0	0	t9
0	0	0	0	0	0	0	0	0	0	0	0	0	0	0	0	0	t10
0	0	0	0	0	0	0	0	0	0	0	0	0	0	0	0	0	t11
0	0	0	0	0	0	0	0	0	0	0	0	0	0	0	0	0	t12
0	0	0	0	0	0	0	0	0	0	0	0	0	0	0	0	0	t13

Matrix 2

CONCLUSIONS

In the field of railway automation and telemechanics, code transmitting devices are modeled on the basis of Petri nets, and the processes occurring in the delivery of existing «G» codes in sections equipped with autoblocking and automatic locomotive signaling are described by the example of Petri graphs. Each described process was studied in the Petri Mathematical Simulator.

USED LITERATURE

1. Soroko V. I., Fotkina Zh. V. Equipment for railway automatics and telemechanics: Reference book: in 4 books. Book. 1. - 4th ed. - M .: LLC «NPF» PLANET «, 2013 - 1060 p.
2. Kazanov A. A. et al. Systems of interval regulation of train traffic / A. A. Kazakov, V. D. Bubnov, E. A. Kazakov: A textbook for railway technical schools. transp. — M.: Transport, 1986. — 399 p.
3. Kazakov A.A., Bubnov V.D., Kazakov E.A. Automated systems for interval control of train traffic: Textbook, for technical schools of the railway. transp. M.: Transport, 1995. - 320 p.
4. Theeg G., and Vlasenko S. «Railway Signaling & Interlocking - International Compendium», Eurailpress, 2009, 448 p.
5. Saitov, A., Kurbanov, J., Toshboyev, Z., & Boltayev, S. (2021). Improvement of control devices for road sections of railway automation and telemechanics. E3S Web of Conferences, 264, 05031. doi:10.1051/e3sconf/202126405031.
6. Azizov, A.R., & Shakirova, F.F. (2020). Method for assessing the diagnosis of the technical condition of an integrated microprocessor pulse generator of railway automation and telemechanics. In IOP Conference Series: Materials Science and Engineering (Vol. 862). Institute of Physics Publishing.https://doi.org/10.1088/1757-899X/862/5/052073
7. Sapozhnikov V.V., Sapozhnikov Vl.V., Efanov D.V., Nikitin D.A. «Berger code generation method with increased efficiency of error detection in data bits» // Electronic Modeling, 2013, vol. 1, p. 35, no. 4, pp. 21-34.
8. Boltayev S.T., Gayubov T.N., Rakhmonov B.B., Kosimova Q.A., Ergashov B.G. The creation of microprocessor controlled modules for AC and DC conductors. Journal of critical reviews (JCR), 2020, 7(17): 2183-2189. 10.31838/jcr.07.17.268
9. S. Boltayev, B.Rakhmonov, O.Muhiddinov, A.Saitov, Z.Toshboyev A block model development for intelligent control of the switches operating apparatus position in the electrical interlocking system. CONMECHYDRO – 2021 E3S Web of Conferences 264, 05043 (2021) https://doi.org/10.1051/e3sconf/202126405043
10. Boltayev S.T., Valiyev S.I., Qosimova Q.A. Improving the Method of Sending Information about the Approach of Trains to Railway Crossings. St. Petersburg Electrotechnical University "LETI", and IEEE Russia North West Section Conference of Russian Young Researchers in Electrical and Electronic Engineering (ElConRus) January 25 - 28, 2022 St. Petersburg, Russia. -Electronic ISBN:978-1-6654-0993-3 CD:978-1-6654-0992-6 Print on Demand(PoD) ISBN:978-1-6654-0994-0, 2022-yil. DOI: 10.1109/ElConRus54750.2022.9755564
11. Boltayev S.T., Abdullaev R.B., Ergashov B.G., Hasanov B.Q. Simulation of a Safe Train Traffic Management System at the Stations. St. Petersburg Electrotechnical University "LETI", and IEEE Russia North West Section Conference of Russian Young Researchers in Electrical and Electronic Engineering (ElConRus) January 25 - 28, 2022 St. Petersburg, Russia. -Electronic ISBN:978-1-6654-0993-3 CD:978-1-6654-0992-6 Print on Demand(PoD) ISBN:978-1-6654-0994-0, 2022-yil. DOI: 10.1109/ElConRus54750.2022.9755616
12. Kovkin, A.N. Methods for constructing non-contact devices for interfacing a control computer complex with executive objects of railway automation systems: dissertation ... candidate of technical sciences: 05.22.08 / Kovkin, Alexey Nikolaevich; [Place of protection: Petersburg. state University of Communications]. - St. Petersburg, 2005. - 188 p.
13. Sapozhnikov V., Sapozhnikov V., Efanov D. and Nikitin D., «Combinational circuits checking on the base of sum codes with one weighted data bit,» Proceedings of IEEE East-West Design & Test Symposium (EWDTS 2014), 2014, pp. 1-9, doi: 10.1109/EWDTS.2014.7027064.
14. https://elektrikexpert.ru/tverdotelnoe-rele.html.
15. D. Nikitin, A. Nikitin, A. Manakov, P. Popov and A. Kotenko, «Automatic locomotive signalization system modification with weight-based sum codes,» 2017 IEEE East-West Design & Test Symposium (EWDTS), 2017, pp . 1-5, doi: 10.1109/EWDTS.2017.8110099.
16. Bose, B., & Lin, DJ (1985). Systematic Unidirectional Error-Detecting Codes. IEEE Transactions on Computers, C-34(11), 1026-1032.https://doi.org/10.1109/TC.1985.1676535
17. Fujiwara, E. (2005). Code Design for Dependable Systems: Theory and Practical Applications. Code Design for Dependable Systems: Theory and Practical Applications (pp. 1–701). John Wiley and Sons.https://doi.org/10.1002/0471792748
18. Hololobova, O., Buriak, S., Havryliuk, V., Skovron, I., & Nazarov, O. (2019). Mathematical modeling of the communication channel between the rail circuit and the inputs devices of automatic locomotive signalization. MATEC Web of Conferences, 294, 03009.https://doi.org/10.1051/matecconf/201929403009
19. Kotov V.E. "Petri Nets" - M. 1984 - pp. 5-8.
20. Peterson J. Theory of Petri nets and system modeling per:, per.ang. - M.: 1984. - 264 p..